

Selective determination of mercury(II) by self-referenced surface-enhanced Raman scattering using dialkyne-modified silver nanoparticles

Yan Kang · Ting Wu · Binxiang Liu · Xuan Wang · Yiping Du

Received: 13 January 2014 / Accepted: 7 April 2014 / Published online: 27 April 2014
© Springer-Verlag Wien 2014

Abstract A novel surface-enhanced Raman scattering (SERS) probe was developed for selective determination of Hg(II) ion. It is based on the use of silver nanoparticles (Ag-NPs) modified with the dialkyne 1,4-diethynylbenzene (DEB). Hg(II) undergoes a very selective chemical reaction with the terminal ethynyl groups to form a $-\text{C}\equiv\text{C}-\text{Hg}-\text{C}\equiv\text{C}-$ linkage which triggers the aggregation of Ag-NPs. This generates numerous hot spots that cause a substantial increase in the intensity of the SERS signal at $2,146\text{ cm}^{-1}$. This large effect was exploited for sensitive quantification of Hg(II) in aqueous solution by rationing the intensities of the (Hg-C \equiv C) peak at $2,146\text{ cm}^{-1}$ and the (C \equiv C)_{free} peak at $2,109\text{ cm}^{-1}$. This self-referenced method is superior to the use of an internal standard. The method also displays excellent selectivity over other metal ions. Under optimal conditions, the rationed signal intensity is related to concentration of Hg(II) in the range between 1.1 nM and 61.2 nM, with a detection limit at 0.8 nM. The method was successfully applied to the determination of Hg(II) in spiked samples of river water.

Keywords Mercury ion · Surface-enhanced Raman scattering · Sensor · Diethynylbenzene

Electronic supplementary material The online version of this article (doi:10.1007/s00604-014-1259-9) contains supplementary material, which is available to authorized users.

Y. Kang · T. Wu · B. Liu · X. Wang · Y. Du (✉)
Shanghai Key Laboratory of Functional Materials Chemistry, and
Research Centre of Analysis and Test, East China University of
Science and Technology, Shanghai 200237, Peoples Republic of
China
e-mail: yipingdu@ecust.edu.cn

Introduction

Materials containing mercury element, such as metallic mercury (Hg^0), inorganic mercury (Hg^{2+}) and organic mercury, are highly toxic and have deleterious effects on human health [1]. Inorganic mercury can be formed as a metabolite of other forms of mercury in the brain where it can remain for many years, which can drastically accumulate in fish and concentrate through the food chain by bioamplification, subsequent ingestion by human beings and, consequently, it does great harm to human body. For example, inorganic mercury compounds are responsible for kidney damage [2]. Therefore, concerns over toxic exposure to mercury have motivated the exploration of cost-effective, rapid, facile and reliable method for monitoring Hg^{2+} in biology and environment. There are lots of techniques for detection of mercury, including inductively coupled plasma mass spectrometry (ICP-MS) [3], colorimetric detection [4], fluorimetric method [5], chemiluminescence [6], surface-enhanced Raman scattering (SERS) etc. [7–9]. The method of ICP-MS requires sophisticated instrumentation and complicated sample preparation processes. It is also under the risk of contaminating the instrument by the residual mercury. Additionally, the methods of fluorescence, colorimetric and chemiluminescence always show broad and structureless signals. SERS is an alternative which is not only able to detect the existence of analyte but also provides structural information according to its unique Raman fingerprint of the molecule, offering a promising approach for simple and rapid tracking of mercury ions in biological and environmental systems.

SERS is an extremely sensitive analytical technique mainly based on the giant electromagnetic enhancement induced by metal nanoparticles (NPs), while it cannot directly detect monoatomic species which lack vibrational signatures, unless they are chemically bound to SERS-active molecules.

Previously reported SERS-based sensors for monoatomic species were based on functionalized nanoparticles, including As^{3+} [10], Cu^{2+} [11], Cd^{2+} [12], Pd^{2+} [13], Hg^{2+} [14] and so on, among which the detection of mercury ions has been widely examined with aptamer [15–17] or organic molecule as recognition probes [18–20]. Recognition of Hg^{2+} by aptamer was based on thymine- Hg^{2+} -thymine coordination chemistry. However, it is laborious and expensive for labeling oligonucleotide with Raman-active dye to obtain SERS signal. The response signals of many organic molecule-based sensors were susceptible to interference substances. Meanwhile, $\text{Hg}(\text{II})$ often coexists with other ions. Therefore, selectivity in detection of Hg^{2+} is of crucial significance. These demands in monitoring mercury ions would require new strategies and simple sensing systems to analyze them selectively and fast against other interference metal ions.

In this assay, we present an acetylene derivative, 1,4-diethynylbenzene (DEB), with two pendent terminal ethynyl groups. DEB is a SERS-active substance, capable of binding to the surface of Ag-NPs via one of its terminal ethynyl groups [21–23]. Meanwhile, in the presence of Hg^{2+} , DEB coordination with Hg^{2+} afforded $\text{C} \equiv \text{C}-\text{Hg}-\text{C} \equiv \text{C}$ linkage, which shortened the distances among the Ag-NPs modified with DEB (DEB-Ag-NPs) [24, 25]. In this case, Hg^{2+} acted as bridges to link DEB-Ag-NPs together, which triggered the aggregation of Ag-NPs, thus generating lots of hot spots with a substantial turn-on of SERS signal. In particular, it was found in this work that the vibrational profiles of DEB were sensitive to the presence of mercury ions. A distinct vibrational signature of $\text{C} \equiv \text{C}-\text{Hg}-\text{C} \equiv \text{C}$ at $2,146 \text{ cm}^{-1}$ was observed, which located in the Raman spectrally silent window ($1,900\text{--}2,500 \text{ cm}^{-1}$), unique to many other background interference. This observation offered us a chance to obtain a SERS-based quantification of Hg^{2+} in aqueous solution. In addition, contrasting response was adopted by selecting vibrational bands in the SERS profiles, allowing direct quantitative assays of Hg^{2+} by employing intensity ratios of two bands instead of using internal standards. The aforementioned points were favorable for analysis of Hg^{2+} . In addition to the trace detection of mercury ions, the SERS technique affords valuable structural information about the reaction mechanism between mercury ions and terminal ethynyl groups.

Experimental

Materials and reagents

Silver nitrate, sodium citrate, DEB and all metallic salts used in this study were obtained from Sinopharm Chemical Reagent Co., Ltd (Shanghai, China, <http://www.sinoreagent.com/>) without further purification. All other chemicals used were of analytical grade. All solutions were prepared with ultrapure water ($18.2 \text{ M}\Omega \text{ cm}^{-1}$) obtained from a purification system

(SARTORIUS arium 611 DI, Germany, <http://www.sartorius.com.cn/>). Certified reference material of mercury GBW (E) 080,392 “mercury in simulated natural water” was purchased from Beijing Yihua Standard Technology Co. Ltd (Beijing, China, <http://www.chem17.com/Company/Detail/252784.html>).

Preparation of Ag-NPs

Ag-NPs were prepared by reducing silver nitrate using sodium citrate [26]. In a typical experiment, 18 mg AgNO_3 was dissolved in 100 mL of H_2O and brought to boiling. A solution of 1 % sodium citrate (2 mL) was added. The solution was kept on boiling for ca. 1 h. The prepared silver colloid was stored at $-4 \text{ }^\circ\text{C}$. The colloids were rinsed with water and ethanol for 3 times and were resuspended in water by ultrasonication. The concentrated colloidal suspension was then diluted in $18 \text{ M}\Omega \text{ H}_2\text{O}$. UV–Vis spectroscopy and dynamic light scattering (DLS) were used to characterize the particle size of the colloids.

SERS detection of Hg^{2+}

Various concentrations of Hg^{2+} solution were prepared using serial dilution of the stock solution. The SERS detections of aqueous Hg^{2+} were performed at ambient temperature ($22 \text{ }^\circ\text{C}$). $500 \text{ }\mu\text{M}$ ethanol solution of DEB was freshly prepared, then $50 \text{ }\mu\text{M}$ DEB ($\text{pH} = 9$) was obtained by diluting the ethanol solution with basic water. In a typical experiment, Ag-NPs were functionalized with DEB by incubating $100 \text{ }\mu\text{L}$ of $50 \text{ }\mu\text{M}$ DEB with $100 \text{ }\mu\text{L}$ Ag sol for 5 min at ambient temperature ($22 \text{ }^\circ\text{C}$). And then $10 \text{ }\mu\text{L}$ of Hg^{2+} standard solution with variable concentrations was added to $200 \text{ }\mu\text{L}$ of DEB-Ag-NPs. SERS measurements were carried out after DEB-Ag-NPs reacting with Hg^{2+} for 10 min.

Instrumentation and characterization

UV–Vis absorption spectroscopic measurements were carried out using a Cary 500 spectrophotometer with 2 mm path-length cells (Varian, USA, <http://www.varian.com/>). Photographs of the solutions were taken with Canon 530A digital camera (Japan). Raman and SERS experiments were conducted using a Renishaw InVia Reflex confocal microscope (Renishaw, UK, <http://www.renishaw.com.cn/zh/1030.aspx>) equipped with a $50\times$ objective and a high-resolution grating with $1,800 \text{ grooves/cm}$. SERS spectra were acquired using 514.5 nm as the excitation wavelength with exposure times of 10 s. The DLS diameters of the samples were measured using a Nicomp TM 380 ZLS zeta-potential/particle sizer (PSS Nicomp particle size system, USA, <http://www.pssnicomp.cn/>).

Results and discussions

Mechanism for the sensing system

Figure 1 illustrates explicitly the sensing mechanism. A coordination reaction between Hg^{2+} and DEB occurred via a deprotonation process on its terminal ethynyl group, affording $\text{C}\equiv\text{C}-\text{Hg}-\text{C}\equiv\text{C}$ linkage (Fig. 1a) [24, 25]. Fig. 1b displays the schematic diagram of mechanism for the detection of Hg^{2+} with DEB-Ag-NPs. When DEB was added to the Ag-NPs, one of its ethynyl groups would bind to the surface of Ag-NPs [22]. In the present study, Ag-NPs kept yellow after the addition of 5×10^{-5} M DEB, indicating that the DEB-Ag-NPs kept well stabilized in the presence of low concentration of DEB (Fig. 2 inset). Upon addition of Hg^{2+} to the DEB-Ag-NPs, the formation of $-\text{C}\equiv\text{C}-\text{Hg}-\text{C}\equiv\text{C}-$ linkage led to dramatic aggregation of Ag-NPs, as evidenced by a new peak of alkyne group on Raman spectra (Fig. 4), which was in good accordance with some previous reports [24, 25]. Concomitantly, the color of Ag-NPs sol changed from yellow to deep grey gradually with the concentration of metal ions increasing (Fig. 2 inset). In this case, it is reasonable to presume that Hg^{2+} acted as bridges to link the DEB-Ag-NPs together, which accordingly caused their aggregations. As a matter of fact, hot spots can be naturally generated through the aggregation process and localized in the region between two interacting nanoparticles where the electric field is strongly intensified, thus leading to a strong SERS signal of reporter. The mechanism is further confirmed by UV-Vis (Fig. 2) absorption spectroscopy and dynamic light scattering (Fig. 3). The key issue to the current method is the fact that the presence of Hg^{2+}

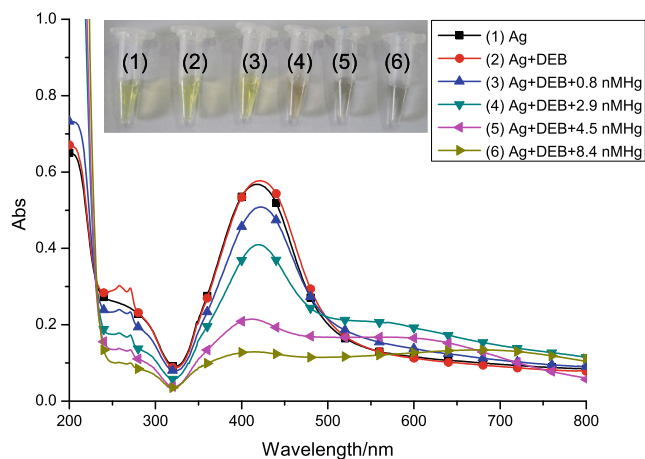


Fig. 2 The UV-Vis spectra of Ag-NPs as well as DEB-Ag-NPs in the presence of different concentrations of Hg^{2+} . Inset: corresponding photographic images

triggers the aggregation of nanoparticles and this behavior is essential for generating SERS signal. More importantly, a characteristic vibrational signal of $-\text{C}\equiv\text{C}-\text{Hg}-\text{C}\equiv\text{C}-$ at $2,146\text{ cm}^{-1}$ is obtained. Accordingly, a sensing platform for detecting Hg^{2+} has been established based on this characteristic signal.

Confirmation of the aggregation of DEB-Ag-NPs by UV-Vis and DLS

The unmodified silver sol is yellow and transparent, indicating good dispersity of Ag-NPs in water (Fig. 2 inset). The UV-Vis absorption spectra (Fig. 2) of Ag-NPs show a typical and

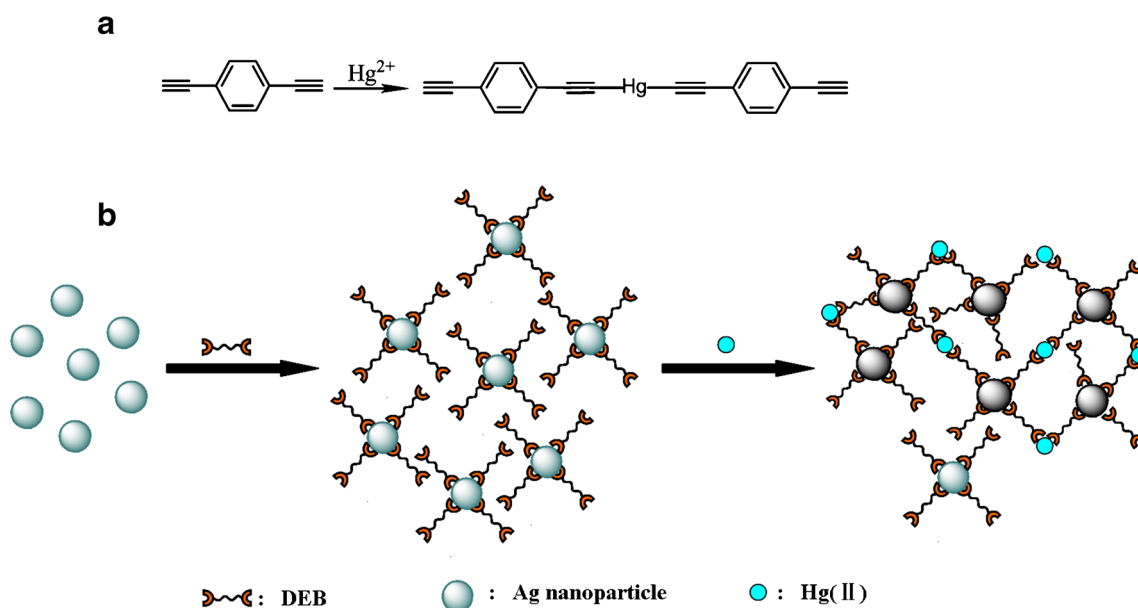


Fig. 1 **a** Schematic representation of the binding of Hg^{2+} with DEB (adsorbed on Ag nanoparticles). **b** schematic diagram of the direct sers method for measuring hg^{2+} using deb-ag-nps. when hg^{2+} ions were added to the system, the binding of Hg^{2+} with DEB caused the aggregation of Ag-NPs

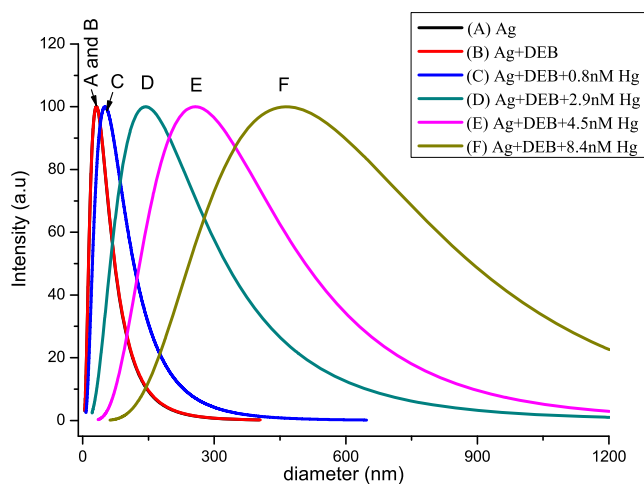


Fig. 3 Dynamic-diameter distribution curves of Ag-NPs as well as DEB-Ag-NPs in the presence of different concentrations of Hg^{2+} , which were obtained by dynamic light scattering

intense absorption peak (around 420 nm) due to the surface plasmon excitation [27]. When Ag-NPs are mixed with DEB (5×10^{-5} M), no obvious shift of the localized plasmon resonance band is observed. Meanwhile, no evidence of agglomeration is observed in the electronic spectrum. In particular, the photographic image (Fig. 2 inset (2)) also shows the DEB-Ag-NPs sol is yellow and well-dispersed. After addition of DEB to the Ag-NPs sol, some new features in the structure of adsorbate make another double peak around 275 nm of DEB observable (Fig. 2). The absorption peak is assigned to K-band of DEB, with ϵ (molar absorptivity) max as high as 9×10^4 . Upon addition of Hg^{2+} , a regular decrease in the absorbance of Ag-NPs at 420 nm is observed with the concentration of metal ion increasing, which indicates the aggregation of Ag-NPs induced by Hg^{2+} . Furthermore, the intensity of a new absorption band at ca. 580 nm also changes with the variable concentrations of Hg^{2+} , which is associated with the presence of aggregates, particularly chainlike aggregates [28]. The above observations give another evidence to support the mechanism of the sensor. Similarly, with an increase in the concentration of Hg^{2+} , a visual color changes from yellow to deep grey (Fig. 2 inset). The noticeable transformations in UV-Vis spectra of Ag-NPs and visual color changes of photographic images demonstrate the aggregation of DEB-Ag-NPs induced by Hg^{2+} .

DLS measurements were carried out in order to examine the Hg^{2+} -induced changes in hydrodynamic radius distribution of Ag-NPs (Fig. 3). For the freshly prepared Ag colloids and DEB-Ag-NPs, the two plots of their size distribution almost overlap, indicating that Ag-NPs could keep stable in the presence of low concentration of DEB. After the addition of Hg^{2+} , the increase in average hydrodynamic radius suggests the continual growth of aggregates with the increase of concentration of Hg^{2+} [29]. These results are quite consistent with the conclusions obtained by the UV-Vis spectra.

Changes of the diameters obtained from DLS evidence the linkage of mercury ions with ethynyl group, thus leading to the aggregation of Ag-NPs.

Raman and SERS spectra of DEB and DEB-Hg

Raman spectra of 0.02 M and solid DEB are shown in Fig. 4 b and c, respectively. There are no obvious differences of the Raman shifts between these two spectra. The Raman modes for DEB have been assigned previously and the observed vibrational frequencies are listed in Table S1 (Electronic Supplementary Material, ESM) along with the appropriate vibrational assignments [21, 30]. A detailed analysis of the SERS of DEB (Fig. 4) shows marked changes in both the intensity of bands and the peak positions in comparison to the normal Raman spectra. In the range from 1,000 to 2000 cm^{-1} , the prominent features in Fig. 4 are the in-plane ring modes at 1,171 and 1,596 cm^{-1} . From Fig. 4a and b, and Table S1 (ESM), it can be seen that the peak at 1,171 cm^{-1} exhibits only a slight change in its position and bandwidth upon surface adsorption between the Raman and SERS spectra. These observations indicate that the phenyl group of DEB doesn't interact strongly with the silver surface and may stand vertical on the surface [31]. The binding of DEB to Ag-NPs induces noticeable shifts of the bands associated with stretching vibrational modes of $\text{C}\equiv\text{C}$ bond, namely from 2,100 cm^{-1} in the Raman spectrum to a triplet peaks at 1980, 2,109, and 2,212 cm^{-1} in the SERS spectrum. The bands at 1980 cm^{-1} , 2,212 cm^{-1} and 2,109 cm^{-1} are assigned to the stretch of bound $\text{C}\equiv\text{C}$ and free $\text{C}\equiv\text{C}$, respectively [21]. More importantly, the bandwidth of stretch of the $\nu(\text{C}\equiv\text{C})_{\text{bound}}$ at 1980 cm^{-1} becomes broadened upon adsorption. A direct interaction between $\text{C}\equiv\text{C}$ group and Ag-NPs is evidenced

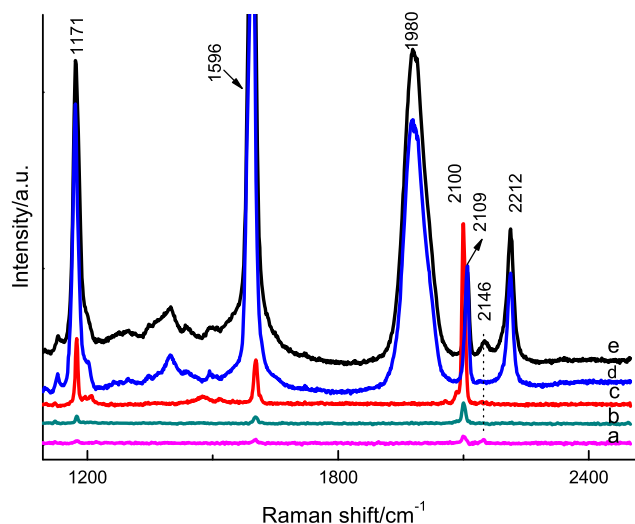


Fig. 4 Raman spectra of a 0.02 M DEB reacted with 5 mM Hg^{2+} , b 0.02 M DEB, c DEB in its solid state. SERS spectra of d 2.5×10^{-5} M DEB on Ag-NPs, and e DEB-Ag-NPs reacted with 1.5 nM Hg^{2+} in the range of 1,000–2,500 cm^{-1}

on the basis of the significant shifts observed in the SERS spectrum of the ν (C \equiv C) stretching mode at 1980, 2,212 and 2,109 cm^{-1} , respectively, in comparison with the normal Raman spectrum. DEB binds to the surface of Ag-NPs mainly via one of its two terminal ethynyl groups, with the other $-\text{C}\equiv\text{CH}$ group being pendent with respect to the silver surface [30, 31]. It is noteworthy that ν (C \equiv C)_{free} in Fig. 4d is found 9 cm^{-1} higher than that in Fig. 4c of the Raman spectrum. This upshift may indicate that the pendent terminal $-\text{C}\equiv\text{CH}$ group of DEB on Ag-NPs is free of any intermolecular hydrogen bonding [30, 32]. The splitting and red shift upon adsorption on the surface of Ag-NPs were consistent with previous reports [30–32].

In the presence of Hg^{2+} , the vibrational modes of ethynyl group of DEB underwent a marked change upon complexation with Hg(II) to give an intense peak centered at 2,146 cm^{-1} , indicating that a Hg(II)-selective SERS signaling behavior occurred. A plausible attribution of this new band is the vibrational mode of $-\text{C}\equiv\text{C}-\text{Hg}-\text{C}\equiv\text{C}-$, which will be discussed in detail in the following. Additionally, a concomitant decrease in the intensity of the peak ν (C \equiv C)_{free} at 2,109 cm^{-1} is also observed. In order to confirm the assignment of the peak at 2,146 cm^{-1} , we mixed 0.02 M DEB with 5 mM Hg^{2+} . Raman spectrum of the mixture is presented in Fig. 4a. Comparing Fig. 4a with b, there are no other obvious differences than a new peak at 2,146 cm^{-1} on the spectrum of the mixture, which strongly indicates that this new vibrational mode is induced by the presence of Hg^{2+} . Therefore, it is reasonable to assign the new band to the vibration mode of $-\text{C}\equiv\text{C}-\text{Hg}-\text{C}\equiv\text{C}-$. These results further support the scheme illustrated in Fig. 1a. A Hg^{2+} -selective SERS signaling system is established on this phenomenon.

The performance of the sensor to Hg^{2+} of varying concentration

The aforementioned section has discussed that the pendent terminal $-\text{C}\equiv\text{CH}$ of DEB-Ag-NPs has high affinity for Hg^{2+} . The coordination of Hg(II) with the DEB moiety generates a characteristic peak at 2,146 cm^{-1} which is distinct from that of pure DEB. The difference between Raman profiles of Hg(II)-DEB and DEB is sufficient to determine the identity of the analyte of interest. It does highlight that there is a systematic decrease of the ν (C \equiv C)_{free} peak at 2,109 cm^{-1} and, concomitantly, a gradual increase of the $\nu_{\text{Hg}-\text{C}\equiv\text{C}}$ peak at 2,146 cm^{-1} upon the metal ion concentration increasing in the range of 1.1–61.2 nM, consistent with the strong binding of Hg^{2+} to the ethynyl groups, as illustrated in Fig. 5. In particular, these trends of SERS signals in response to the augmented concentration of Hg^{2+} ion are in good accordance with the mechanism. Meanwhile, it is worth noting that the multiple trends of the intensities of the peaks at 2,109 cm^{-1} and 2,146 cm^{-1} change as a function of the Hg^{2+} concentration. These changes

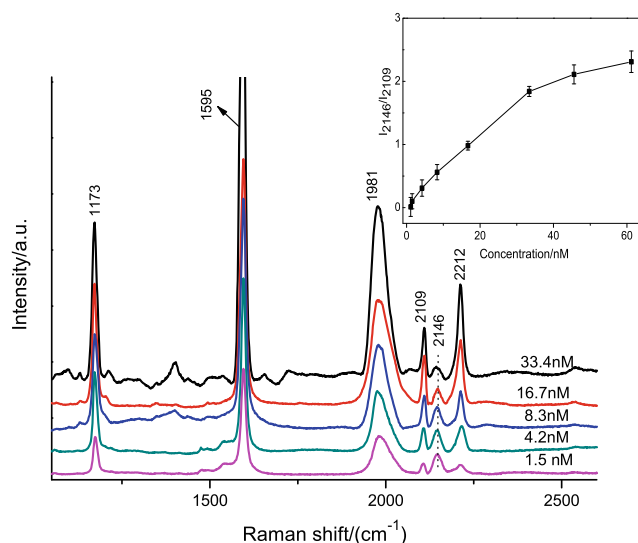


Fig. 5 SERS spectra of DEB-Ag-NPs (2.5×10^{-5} M) response to variable concentrations of Hg^{2+}

are correlated quantitatively with metal ion concentration using ratiometric peak intensities, I_{2146}/I_{2109} . Accordingly, we develop a convenient analytical strategy based on this feature. The effect of reaction time of DEB with Hg^{2+} and pH value of DEB were investigated and an optimum time of 10 min and pH=9 of DEB were chosen for this work (see Fig. S1, ESM). Under optimal condition, the response signals for DEB to variable concentrations of Hg^{2+} were obtained. A plot of I_{2146}/I_{2109} versus analyte concentration is presented in the inset in Fig. 5. The rationed signal intensity is related to concentration of Hg(II) in the range between 1.1 nM and 61.2 nM, with a detection limit at 0.8 nM. Irrespective of the changes of intensity of SERS signal, the fact remains that Hg^{2+} -selective SERS signaling system is well established based on the ratiometric peak intensities, I_{2146}/I_{2109} . This method was used to quantify mercury in GBW (E) 080,392 “mercury in simulated natural water” and an average

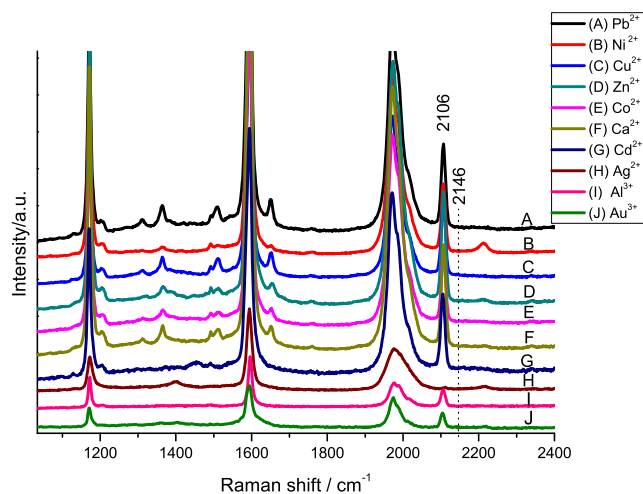


Fig. 6 Response signals of this sensing system to other metal ions

concentration of $9.98 \pm 0.46 \mu\text{g L}^{-1}$ (RSD 4.6 %) was obtained, which was within the certified range $10 \pm 0.5 \mu\text{g L}^{-1}$. In comparison to that of previously reported sensor for Hg^{2+} (see Table S2, ESM), the sensitivity of this method is superior to that of lots of methods [4, 5, 7, 18]. Although some other methods for Hg^{2+} detection, such as chip-based [15] and aptamer-based [6, 14, 16], provide better detection limit, they are limited either by the complexity of the assay or laborious labeling processes. This assay offers several advantages, containing self-referenced, cost-effective and high specificity.

The selectivity of the SERS sensor to other metal ions

Considering the application of this sensing system for environmental analysis, one should pay additional attention to the issue of selectivity. In this assay, the selectivity of this method has been investigated by testing the SERS signal to various metal ions, including Ag^+ , Cu^{2+} , Ni^{2+} , Zn^{2+} , Co^{2+} , Ca^{2+} , Al^{3+} , Pb^{2+} , Cd^{2+} and Au^{3+} at a concentration of $1 \mu\text{M}$. The signals were obtained after previous aggregations of Ag-NPs by adding 0.1 M NaCl . It was observed that the SERS sensor exhibited different response to other metal ions (Fig. 6). As is shown in this figure, there are no peaks at $2,146 \text{ cm}^{-1}$. Besides, the bands of vibration modes of $-\text{C}\equiv\text{CH}$ at $2,106 \text{ cm}^{-1}$ are very strong. These observations demonstrate the excellent selectivity of the current assay towards Hg^{2+} over other metal ions, which is attributed to the specific recognition reaction between $-\text{C}\equiv\text{CH}$ group and Hg^{2+} . These results indicate this sensor has potential to be applied in environmental analysis. The functionalized nanoparticles were employed to test the feasibility for the analysis of practical samples which were collected from a river in Shanghai. As shown in Table S3 (ESM), recoveries of this method are excellent, suggesting that it is promising for the determination of Hg^{2+} in real samples.

Conclusion

In the present work, we have shown a probe of DEB molecular which can bind to Ag-NPs surface through one of its two terminal ethynyl group. Upon addition of Hg^{2+} , each mercury ion could bridge two DEB-Ag-NPs, resulting in the aggregation of Ag-NPs. Accordingly, a great enhancement in SERS signal could be obtained. In particular, the sensing platform can give direct response to the presence of Hg^{2+} , namely a characteristic vibration mode of $\text{Hg}-\text{C}\equiv\text{C}$ appearing at $2,146 \text{ cm}^{-1}$. Experimental results showed that Hg^{2+} could be detected selectively against other competing metal ions. Under optimal assay conditions, analytical range of $1.1\text{--}61.2 \text{ nM}$ was obtained. These noticeable features demonstrated a highly selective and sensitive platform for the detection of Hg^{2+} was successfully fabricated via SERS technique. Its practicality

was validated through analysis of river water sample. This simple, rapid, cost-effective and selective sensing system holds great potential for environmental analysis.

Acknowledgments We are thankful to the National Natural Science Foundation of China (21,205,041) for financial support. The authors are grateful to Dr. J.X. Li, L.F. Zhang, L. Zhang, D.F. Li and W. Tao for helpful discussions.

References

- Clarkson TW, Magos L, Myers GJ (2003) The toxicology of mercury — current exposures and clinical manifestations. *N Engl J Med* 349:1731–1737. doi:10.1056/NEJMra022471
- Magos L, Brown AW, Sparrow S, Bailey E, Snowden RT, Skipp WR (1985) The comparative toxicology of ethyl- and methylmercury. *Arch Toxicol* 57:260–267. doi:10.1007/BF00324789
- Lynam MM, Klaue B, Keeler GJ, Blum JD (2013) Using thermal analysis coupled to isotope dilution cold vapor ICP-MS in the quantification of atmospheric particulate phase mercury. *J Anal Spectrom* 28:1788–1795. doi:10.1039/c3ja50184a
- Chansuvarn W, Imyim A (2012) Visual and colorimetric detection of mercury (II) ion using gold nanoparticles stabilized with a dithiadiazia ligand. *Microchim Acta* 176:57–64. doi:10.1007/s00604-011-0691-3
- Cao B, Yuan C, Liu B, Jiang C, Guan G, Han MY (2013) Ratiometric fluorescence detection of mercuric ion based on the nanohybrid of fluorescence carbon dots and quantum dots. *Anal Chim Acta* 786:146–152. doi:10.1016/j.aca.2013.05.015
- Cai S, Lao K, Lau C, Lu J (2011) “Turn-On” chemiluminescence sensor for the highly selective and ultrasensitive detection of Hg^{2+} ions based on interstrand cooperative coordination and catalytic formation of gold nanoparticles. *Anal Chem* 83:9702–9708. doi:10.1021/ac202789q
- Chen Y, Wu L, Chen Y, Bi N, Zheng X, Qi H, Qin M, Liao X, Zhang H, Tian Y (2012) Determination of mercury (II) by surface-enhanced Raman scattering spectroscopy based on thiol-functionalized silver nanoparticles. *Microchim Acta* 177:341–348. doi:10.1007/s00604-012-0777-6
- Li DW, Zhai WL, Li YT, Long YT (2013) Recent progress in surface enhanced Raman spectroscopy for the detection of environmental pollutants. *Microchim Acta*. doi:10.1007/s00604-013-1115-3
- Chen S, Liu D, Wang Z, Sun X, Cui D, Chen X (2013) Picomolar detection of mercuric ions by means of gold–silver core–shell nanorods. *Nanoscale* 5:6731–6735. doi:10.1039/c3nr01603j
- Li J, Chen L, Lou T, Wang Y (2011) Highly sensitive SERS detection of As^{3+} ions in aqueous media using glutathione functionalized silver nanoparticles. *ACS Appl Mater Interfaces* 3:3936–3941. doi:10.1021/am200810x
- Sarkar S, Pradhan M, Sinha AK, Basu M, Pal T (2012) Selective and sensitive recognition of Cu^{2+} in an aqueous medium: a surface-enhanced Raman scattering (SERS)-based analysis with a low-cost Raman reporter. *Chem Eur J* 18:6335–6342. doi:10.1002/chem.201103458
- Yin J, Wu T, Song J, Zhang Q, Liu S, Xu R, Duan H (2011) SERS-active nanoparticles for sensitive and selective detection of cadmium ion (Cd^{2+}). *Chem Mater* 23:4756–4764. doi:10.1021/cm201791r
- Wang Y, Irudayaraj J (2011) A SERS DNzyme biosensor for lead ion detection. *Chem Commun* 47:4394–4396. doi:10.1039/COCC04140H

14. Zhang L, Chang H, Hirata A, Wu H, Xue QK, Chen M (2013) Nanoporous gold based optical sensor for sub-ppt detection of mercury ions. *ACS Nano* 7:4595–4600. doi:10.1021/nm4013737
15. Chung E, Gao R, Ko J, Choi N, Lim DW, Lee EK, Chang SI, Choo J (2013) Trace analysis of mercury (II) ions using aptamer modified Au/Ag core-shell nanoparticles and SERS spectroscopy in a microdroplet channel. *Lab Chip* 13:260–266. doi:10.1039/c2lc41079f
16. Ma W, Sun M, Xu L, Wang L, Kuang H, Xu C (2013) A SERS active gold nanostar dimer for mercury ion detection. *Chem Commun* 49:4989–4991. doi:10.1039/C3CC39087J
17. Kang T, Yoo SM, Kang M, Lee H, Kim H, Lee SY, Kim B (2012) Single-step multiplex detection of toxic metal ions by Au nanowires-on-chip sensor using reporter elimination. *Lab Chip* 12:3077–3081. doi:10.1039/C2LC40185A
18. Duan J, Yang M, Lai Y, Yuan J, Zhan J (2012) A colorimetric and surface-enhanced Raman scattering dual-signal sensor for Hg²⁺ based on Bismuthiol II-capped gold nanoparticles. *Anal Chim Acta* 723:88–93. doi:10.1016/j.aca.2012.02.031
19. Li P, Liu H, Yang L, Liu J (2013) Sensitive and selective SERS probe for Hg(II) detection using aminated ring-close structure of rhodamine 6G. *Talanta* 106:381–387
20. Li F, Wang J, Lai Y, Wu C, Sun S, He Y, Ma H (2013) Ultrasensitive and selective detection of copper (II) and mercury (II) ions by dye-coded silver nanoparticle-based SERS probes. *Biosens Bioelectron* 39:82–87. doi:10.1016/j.bios.2012.06.050
21. Yoo BK, Joo SW (2007) In situ raman monitoring triazole formation from self-assembled monolayers of 1,4-diethynylbenzene on Ag and Au surfaces via “click” cyclization. *J Colloid Interface Sci* 311:491–496. doi:10.1016/j.jcis.2007.02.036
22. Kennedy DC, McKay CS, Tay LL, Rouleau Y, Pezacki JP (2011) Carbon-bonded silver nanoparticles: alkyne-functionalized ligands for SERS imaging of mammalian cells. *Chem Commun* 47:3156–3158. doi:10.1039/c0cc05331g
23. Kennedy DC, Hoop KA, Tayc LL, Pezacki JP (2010) Development of nanoparticle probes for multiplex SERS imaging of cell surface proteins. *Nanoscale* 2:1413–1416. doi:10.1039/C0NR00122H
24. Fabbri D, Lombardo M, Trombini C, Vassura L (1995) A new procedure for the speciation of mercury in water based on the transformation of mercury (II) and methylmercury (II) into stable acetylides followed by HPLC analysis. *Appl Organomet Chem* 9:713–718. doi:10.1002/aoc.590090810
25. Bolletta F, Fabbri D, Lombardo M, Prodi L, Trombini C, Zaccheroni N (1996) Synthesis and photophysical properties of fluorescent derivatives of methylmercury. *Organometallics* 15:2415–2417. doi:10.1021/om950793b
26. Lee PC, Meise D (1982) Adsorption and surface-enhanced raman of dyes on silver and gold sols. *J Phys Chem* 86:3391–3395. doi:10.1021/j100214a025
27. Joo SW, Kim K (2004) Adsorption of phenylacetylene on gold nanoparticle surfaces investigated by surface-enhanced Raman scattering. *J Raman Spectrosc* 35:549–554. doi:10.1002/jrs.1183
28. Sliman O, Bumm LA, Callaghan R, Blatchford CG, Kerker M (1983) Surface-enhanced raman scattering by citrate on colloidal silver. *J Phys Chem* 87:1014–1023. doi:10.1021/j100229a020
29. Tan Y, Jiang L, Li Y, Zhu D (2002) One dimensional aggregates of silver nanoparticles induced by the stabilizer 2-mercaptobenzimidazole. *J Phys Chem B* 106:3131–3138. doi:10.1021/jp012668l
30. Lim JK, Joo SW, Shin KS (2007) Concentration dependent raman study of 1,4-diethynylbenzene on gold nanoparticle surfaces. *Vib Spectrosc* 43:330–334. doi:10.1016/j.vibspec.2006.04.006
31. Lee TW, Kim K, Kim MS (1992) Raman spectroscopy of phenylacetylene adsorbed on silver surfaces. *J Mol Struct* 274:59–73. doi:10.1016/0022-2860(92)80146-9
32. Joo SW, Han SW, Kim K (1999) Adsorption characteristics of p-Xylene- α , α' -dithiol on gold and silver surfaces: surface-enhanced Raman scattering and ellipsometry study. *J Phys Chem B* 103:10831–10837. doi:10.1021/jp99223